PIER Letters

A Broadband SIW Cavity-Backed Circular Arc-Shaped Slot Antenna for Millimeter-Wave Applications

Mingming Gao[1,2], Chunli Liu[1,2,*], Jingchang Nan[1,2], and Hongliang Niu[1,2]

[1]*Liaoning Technical University, China*
[2]*Liaoning Key Laboratory of Radio Frequency and Big Data for Intelligent Applications, China*

ABSTRACT: A broadband circular arc-shaped slot antenna is proposed in this paper which operates from 25.1 GHz to 31.5 GHz. The antenna is based on a substrate-integrated waveguide (SIW) and fed through a grounded coplanar waveguide (GCPW). A circular arc-shaped slot is presented instead of a conventional narrow rectangular slot to extend bandwidth performance. The slot antenna generates six closely resonant frequencies by exciting high-order modes, which help get a broadband response. Antenna's prototype is fabricated using the standard Printed Circuit Board (PCB) process. The results of its measurement show that the antenna achieves an impedance bandwidth of 22.6% at 28 GHz and a peak gain of 11.5 dBi. The efficiency in the operating bandwidth is more than 85%. The antenna shows the merits of low-profile, high-gain, and broadband characteristics, which are very suitable for mm-wave wireless communication systems.

1. INTRODUCTION

With the arrival of the Internet of Things era, more terminal equipment is required, and the spectrum resources of the middle and low-frequency end have made it challenging to meet the application requirements of high-speed data flow in modern wireless communication systems. Millimeter wave frequency band has recently become a hot research topic because of its rich spectrum resources, which can achieve large bandwidth, high speed, and extremely low delay [1, 2]. More and more experts and scholars have devoted themselves to the research of millimeter wave communication, and millimeter wave antennas have also received extensive attention from academia and industry [3, 4].

Slot antennas are widely used in wireless communication and radar systems because of their simple structure, good radiation efficiency, and easy conformity [5]. However, the traditional microstrip slot antenna has the problems of significant transmission loss, substantial radiation interference, and low efficiency in the millimeter wave band. Meanwhile, the high-profile structure of the waveguide slot antenna is challenging to integrate with other planar circuits. Introducing the substrate-integrated waveguide (SIW) structure into the planar slot antenna design can solve the above problems effectively. SIW has been widely used in millimeter-wave circuit design since it was proposed [6], because of its high power capacity, easy integration, and other advantages. It has broad application prospects in millimeter wave and terahertz frequency ranges. However, due to the high-quality factor characteristic of the SIW cavity, the SIW back-cavity slot antenna impedance bandwidth is very narrow [7, 8], which cannot meet the application requirements of a broadband millimeter wave wireless communication system.

Experts and scholars have done much related research to expand the impedance bandwidth of SIW antennas. Currently, the common methods to extend the bandwidth of SIW antennas include changing the slot shape [9–12], loading shorting vias beside the slot [13–15], exciting higher-order modes or mixed modes [16, 17], and introducing multilayer structures with coupled feeders [18, 19]. References [9, 10] extend the bandwidth by replacing the traditional rectangular slot with different shapes, such as double T-shaped slot and venus-shaped slot. However, only less than 10% of the operating bandwidth is realized. Li et al. achieved a broadband of 15.2% by introducing a bow-tie-shaped slot [11]. Based on this, [12] proposes a modified dumbbell-shaped slot with a multi-branch structure to extend the antenna bandwidth to 26.7%. In [13–15], shorting vias are loaded beside the slots to expand impedance bandwidth. Reference [16] combines the above multiple methods of bandwidth expansion by removing part of the metal perforations and introducing multiple slots to enable multiple mixed modes to resonate together, achieving an operating bandwidth of 13.4%. Reference [17] achieves an impedance bandwidth of 42.86% by wide-cavity selected to generate higher modes, producing six resonant points in the D-band. However, it achieves a low gain. In [18], a 36.2% impedance bandwidth is achieved using a multilayer structure with an SIW cavity feed-coupled patch. Reference [19] uses a multilayer structure with an empty SIW cavity to achieve a bandwidth of 40.8%. However, the multilayer structures in [18, 19] cannot be easily integrated with planar structures, limiting their applications, so broadband millimeter-wave antennas with low-profile characteristics are of great research interest.

This work proposes a broadband SIW cavity-backed circular arc-shaped slot antenna with high gain characteristics. By combining the circular arc-shaped slot with the multi-mode res-

---

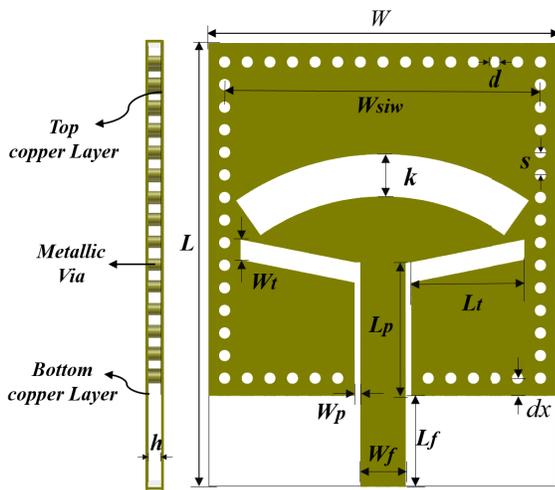* Corresponding author: Chunli Liu (chunli9829@163.com).

FIGURE 1. Configuration of the proposed antenna.

FIGURE 2. Simulated reflection coefficient and gain of the proposed antenna.

onance characteristic of the SIW cavity, under the joint action of the circular arc-shaped and inclined slots of the GCPW structure, the measurement bandwidth of 22.6% is realized, which can be applied to the wireless communication system covering the n257 band. It is a good unit candidate for the millimeter wave array antenna.

2. ANTENNA DESIGN AND ANALYSIS

2.1. Configuration and Performance

The antenna geometry is shown in Fig. 1. In the millimeter-wave band of 28 GHz, Rogers-Duroid 5880 features extremely low dielectric loss, making it ideal for high frequency and wide-band design applications that require minimal dispersion and loss. Therefore, the antenna is fabricated on a 0.787 mm thick single-layer dielectric substrate (Rogers RT5880) with a dielectric constant of 2.2. The SIW resonator consists of two layers of metal plates and a metalized hole with a periodic structure. The circular arc-shaped slot is etched on top of the resonator as the radiation structure of the antenna, and the ground coplanar waveguide (GCPW) structure is used to convert the microstrip wire feed into the SIW. The antenna model is optimized by CST simulation software to obtain the maximum impedance bandwidth. The antenna size is $20\,\text{mm} * 24.5\,\text{mm} * 0.787\,\text{mm}$.

The idea of using the circular arc-shaped slot comes from the evolution process of a rectangular slot into a dumbbell-shaped slot with broadband performance. The antenna's effective length is increased by using the circular arc-shaped slot to obtain the maximum electric field disturbance. In the initial design, the transverse length of the circular arc-shaped slot is set to $2/3 Wsiw$ (where $Wsiw$ is the width of the SIW cavity, equal to 18 mm), and the corresponding circular arc-shaped Angle (ang) is about $60°$. The width (k) is set to 2 mm, which is mainly used for impedance matching.

Figure 2 shows the simulation results of the reflection coefficient and gain of the proposed antenna. It has a $-10\,\text{dB}$ impedance bandwidth of 20.9% (25.3 to 31.2 GHz). Six res-
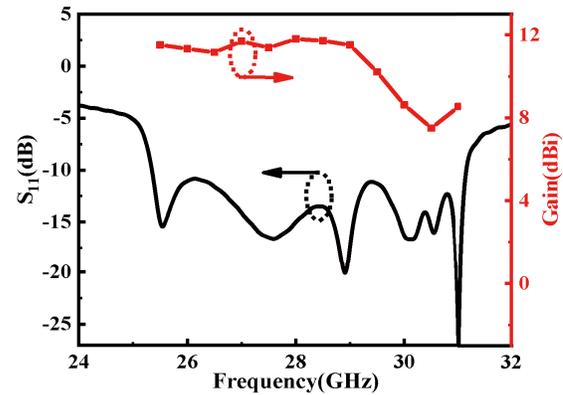
onances are observed clearly in the simulated reflection coefficient. It can be seen from the figure that the antenna gain changes in the range of 7.5–11.5 dBi over the entire bandwidth. In order to explain the broadband operation principle of the proposed antenna, the antenna's design process and structure parameters are analyzed, respectively.

2.2. Working Principle and Design

Compared with the conventional rectangular radiation slot, the circular arc-shaped slot can cut more surface current and excite the high-order modes in the cavity to expand the antenna impedance bandwidth. The TE_{mnl} mode resonant frequency of the SIW cavity can be derived from Equation (1) [20]. However, the size of the antenna SIW cavity proposed in this paper is amplified to excite the high-order modes of the cavity in the operating band.

$$f_{mnl} = \frac{c}{2\pi\sqrt{\mu_r\varepsilon_r}}\sqrt{\left(\frac{m\pi}{a}\right)^2 + \left(\frac{n\pi}{b}\right)^2 + \left(\frac{l\pi}{h}\right)^2} \quad (1)$$

where a, b, and h are the width, length, and height of the SIW resonator. Moreover, m, n, and l represent the number of standing wave changes in each direction. When a and b are equal to w, and the thickness of the substrate is minimal, the Equation (1) can be rewritten into Equation (2):

$$f_{mn0} = \frac{c}{2\pi\sqrt{\mu_r\varepsilon_r}}\sqrt{\left(\frac{m\pi}{w}\right)^2 + \left(\frac{n\pi}{w}\right)^2} \quad (2)$$

In addition, in order to ensure that electromagnetic waves are effectively bound in the SIW, the spacing (s) and diameter (d) of the vias need to be reasonably selected to prevent electromagnetic waves from leaking between the vias. The dimensions of the vias should be calculated according to the conditions $s \leq 2d$ and $d \leq 0.1\lambda_g$ (λ_g is the waveguide wavelength at the center frequency). Finally, the size of the metallization hole $s = 2d$ is selected.
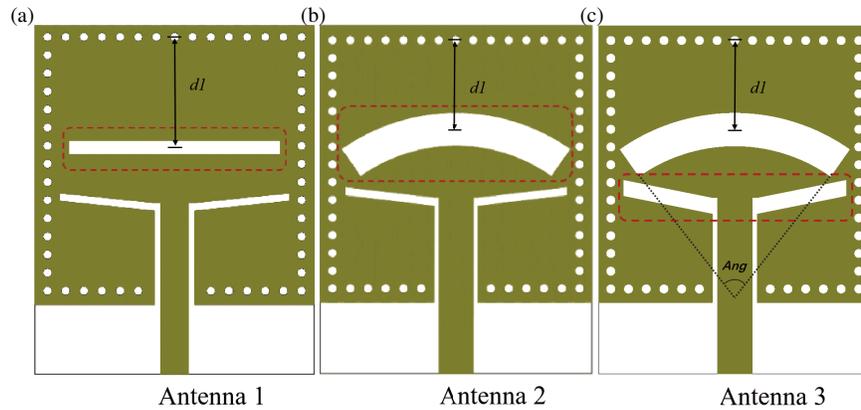
FIGURE 3. The evolution of the traditional rectangular slot [7] to the circular arc-shaped slot antenna.
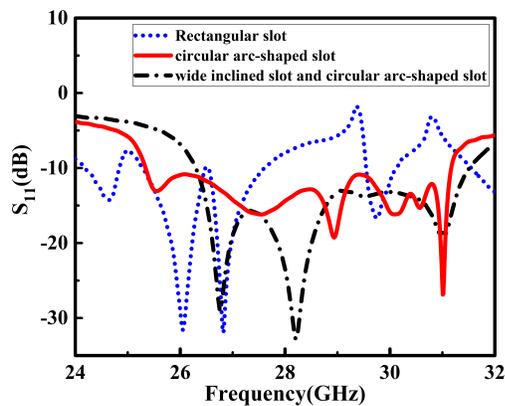

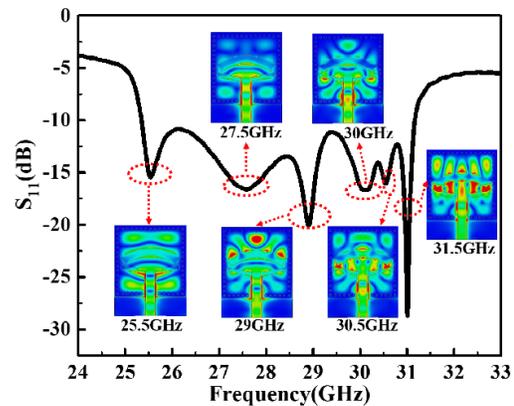**FIGURE 4**. The evolution of the circular-arc slot antenna.

FIGURE 5. Simulated reflection coefficients with E-field distribution at the resonance points.

For SIW back-cavity slot antennas, the impedance bandwidth is determined by the slot's shape and cavity's mode. Fig. 3 shows the design process of the circular arc-shaped antenna. Similar to the traditional rectangular slot antenna [7], Fig. 3(a) shows the rectangular slot initially designed in this paper. The distance between the center of the slot and the short-circuit end of the SIW cavity is $d1$, which is about λ_g. The length of the slot is about $2\lambda_g$. To obtain the maximum disturbance of the electric field, Fig. 3(b) replaces the rectangular slot with a circular arc-shaped slot, and the antenna impedance matching is adjusted by optimizing the angle and width of the circular arc-shaped slot. Fig. 3(c) shows the antenna structure proposed with a wide inclined feed slot of GCPW.

The specific parameters of the three structures were optimized by fine-tuning the circular arc-shaped slot's width and position and the GCPW structure's size. The simulated S_{11} of Antennas 1–3 is illustrated in Fig. 4, exhibiting an impedance bandwidth of 20.9%. By comparison, it can be found that the traditional rectangular slot produces two resonant points close to each other, so the bandwidth is narrow. Meanwhile, introducing the circular arc-shaped slot improves the impedance matching of the antenna at high frequencies. The wide inclined slot of the GCPW structure produces a new resonant point at

the low frequency, further expanding the operating bandwidth.

2.3. Analysis of SIW Mode

This section briefly analyzes the modes of the six resonant frequencies (25.5 GHz, 27.5 GHz, 28.9 GHz, 30.1 GHz, 30.5 GHz, and 31 GHz). Fig. 5 shows the distributions of electric fields corresponding to the six resonant frequencies. The eigenmode simulation of the closed SIW cavity is carried out, and E-field distributions of various modes along with the resonance frequencies are recorded as shown in Fig. 6, which are respectively TE_{140}, TE_{340}, TE_{520}, and TE_{530} in ascending frequency order.

By comparing the field distributions in Fig. 5 and Fig. 6, it can be observed that the electric field distribution in the circular arc-shaped slot cavity is not the standard mode, and the electric field is divided into three parts by the GCPW structure. Meanwhile, the circular arc-shaped slot also disturbs the electric field distribution in the cavity. For a closed SIW cavity, TE_{140} (Fig. 6(a)) mode resonates at 23 GHz, while for the proposed antenna structure in this paper, TE_{140} mode resonates at 25.5 GHz due to the influence of the GCPW structure on the cavity. Similarly, the resonances at 27.5 GHz, 29 GHz, and
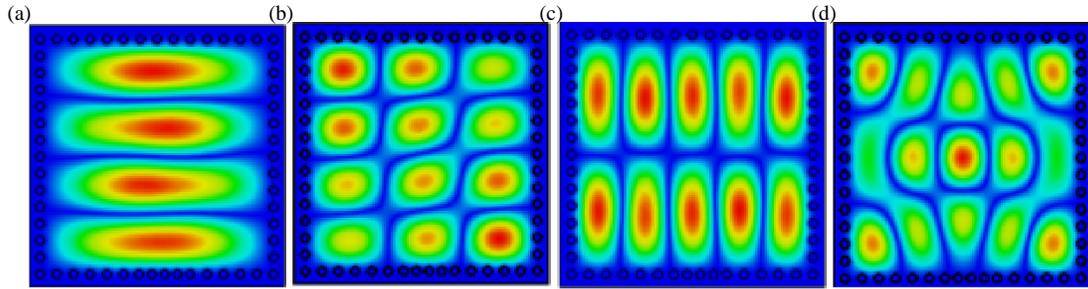
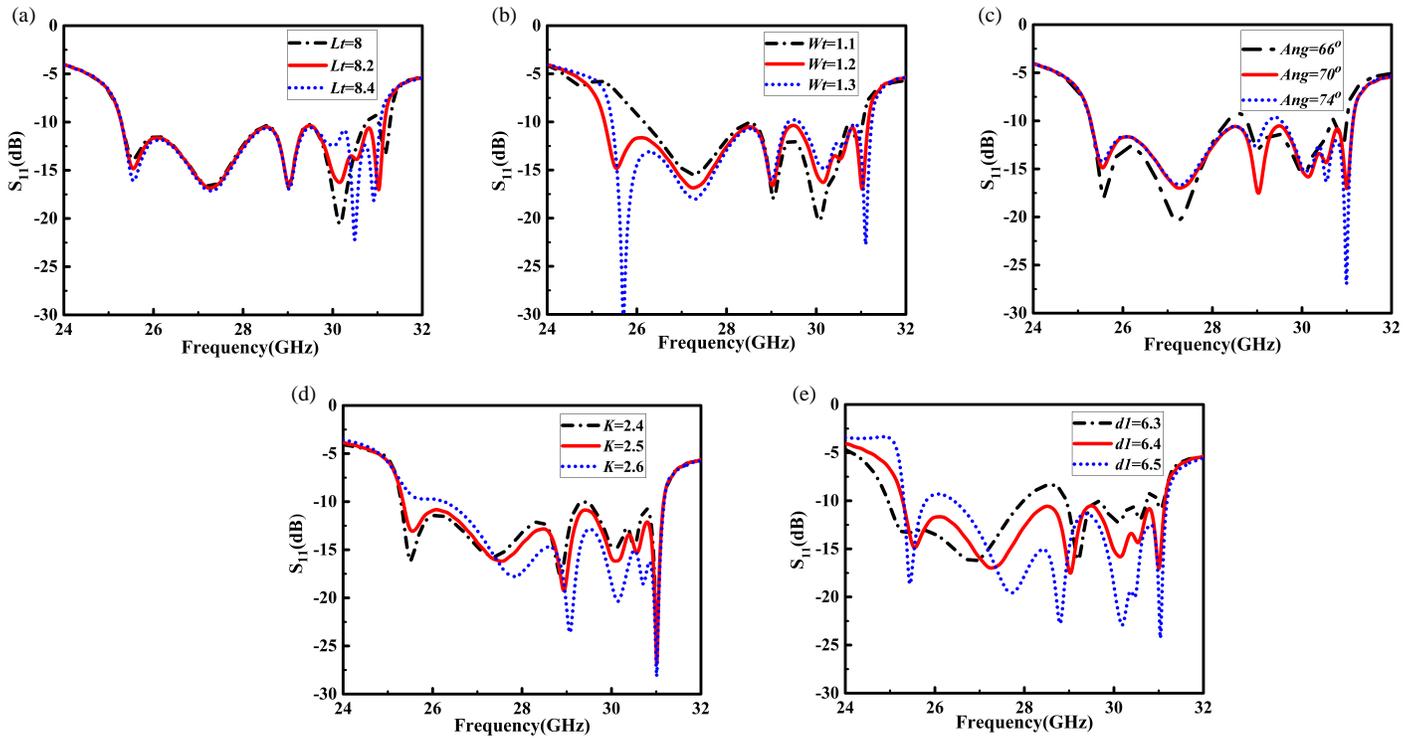**FIGURE 6**. Eigenmode simulation of closed SIW cavity of various modes.

FIGURE 7. Simulated S_{11} with different parameters changed. (a) Length of the inclined slot, Lt. (b) Width of the inclined slot, Wt. (c) Angle of the circular arc-shaped slot, Ang. (d) Width of the circular arc-shaped slot, K. (e) The distance between slot and short-circuit end, $d1$.

30 GHz are all generated by the TE$_{340}$ (Fig. 6(b)) mode. At the frequency of 30.5 GHz, multiple modes are excited simultaneously in the cavity, resulting in a mixed mode. For 31 GHz, the electric field distribution can be seen as generated by TE$_{520}$ and TE$_{530}$ (Fig. 6(c), (d)) modes, and it can be observed that the interaction between the circular arc-shaped slot and the inclined slot of the GCPW mainly generates the radiated electric field at the fifth and sixth resonant frequencies. The appearance of multiple modes is conducive to the expansion of antenna bandwidth.

2.4. Parametric Analysis

Several specific parameters are studied in this section to explain the effect of the circular arc-shaped slot and inclined slot of the GCPW structure on the impedance bandwidth of the proposed antenna.

Figure 7(a) delineates the simulated S_{11} with different Lt. It can be seen that the change of Lt significantly influences the resonant point at the high-frequency end of the antenna. When Lt is 8 mm, it has the best bandwidth but does not meet the requirement of $S_{11} \leq -10$ dB near 31 GHz. When Lt increased from 8 mm to 8.4 mm, the resonant point at the high frequency moved to the low frequency, decreasing bandwidth. In order to obtain the maximum bandwidth while considering the impedance matching at the high-frequency end, Lt has been set to 8.2 mm.

The influence of the width Wt of the inclined slot on antenna S_{11} is shown in Fig. 7(b). Wt mainly determines the first resonance point. With the increase of Wt, a new resonance is generated at the low frequency, and the bandwidth increases, but with the continuous increase of Wt, the bandwidth decreases. Finally, Wt is selected as 1.2 mm.
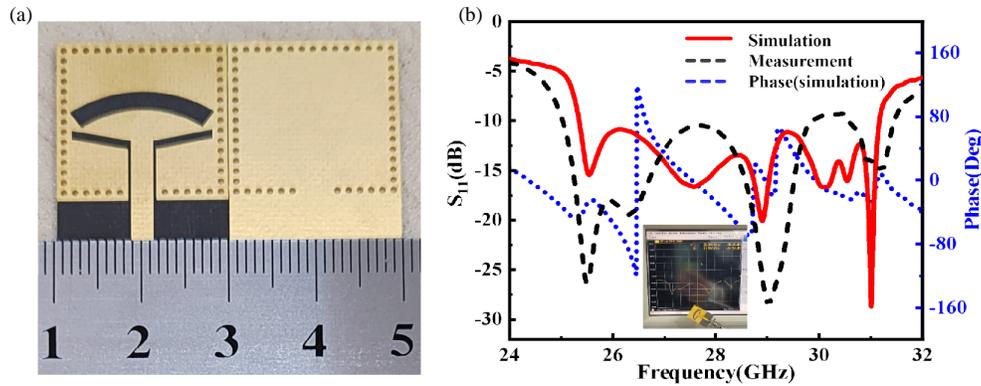
FIGURE 8. Picture and reflection coefficients of the fabricated SIW antenna.

Figure 7(c) shows the S_{11} simulation curve of the circular arc-shaped slot with different angles Ang. The angle size of the slot mainly affects the third resonant frequency. The antenna has the best performance when $Ang = 70°$.

Figure 7(d) shows the effect of slot width K on the simulated S_{11}, which impacts the impedance matching of the antenna in the entire operating bandwidth. With the increase of K, the matching of the low-frequency end becomes worse. Finally, $K = 2.5$ mm is chosen to obtain the best performance.

The influence of $d1$ on the simulated S_{11} is shown in Fig. 7(e). It can be seen that the position of the slot directly affects the resonant mode of the antenna. Hence, the change of the slot position dramatically influences the antenna matching in the whole operating bandwidth. As $d1$ decreases, the second resonant frequency of the antenna moves to the low frequency. After optimizing the $d1$ setting, $d1$ is finally selected as 6.4 mm.

The above analysis shows that the variables Lt and Wt act on the fourth, fifth, sixth, and first resonant frequencies, respectively. The angle of the slot mainly affects the third resonant frequency, and the position and width of the slot affect the overall impedance matching. In addition, the interaction between them is minimal, which is conducive to simplifying antenna design. The optimized antenna parameters are listed in Table 1.

TABLE 1. Geometric dimension of the circular arc-shaped antenna (mm).

Parameter	L	W	$Wsiw$	Wt	Lt
value	24.5	20	18.2	1.2	8.2
Parameter	$d1$	Wp	Lp	Wf	Lf
value	6.4	0.36	7.7	2.57	5.2
Parameter	d	s	Ang	k	dx
value	0.65	1.3	70°	2.5	1

3. MEASUREMENT RESULTS AND DISCUSSION

The antenna prototype was fabricated, and the sample is shown in Fig. 8(a). Fig. 8(b) is the S_{11} curve of simulation and measurement. It can be seen from the measurement results that the first and second resonant points of the antenna move to the low frequency. However, the trends of the simulated and measured curves are basically consistent in the whole working band, and the measured bandwidth is slightly wider than the simulation result, which is about 25.1 GHz–31.5 GHz. It is worth noting that the S_{11} curve deteriorates at 30.1 GHz. It does not meet the requirement of less than -10 dB. The poor correlation between simulation and test results may be caused by the additional loss introduced by the coaxial connector, material losses, and manufacturing tolerances (including the presence of solder and the roughness of the metal surface, and the drift of the dielectric constant at high frequency). Because the resonator is a high-Q resonator, minor deviations can significantly affect the antenna bandwidth.

Figure 9 shows the far-field measurement diagram of the antenna. Fig. 10 shows the simulated and measured E-plane and H-plane radiation pattern results under three different frequencies. The measured and simulated radiation patterns are consistent in the two orthogonal sections. At the high frequency, the circular arc-shaped slot is the main radiation structure, and its forward bending structure leads to the maximum radiation direction deviation of the pattern.

FIGURE 9. The picture of antenna far-field measurement.

Simulation and measurement of antenna gain and efficiency are shown in Fig. 11. The simulation and measurement results have a high agreement and a relatively stable gain in the range of 25.5 GHz–29 GHz. Around 29.5 GHz, the gain begins to
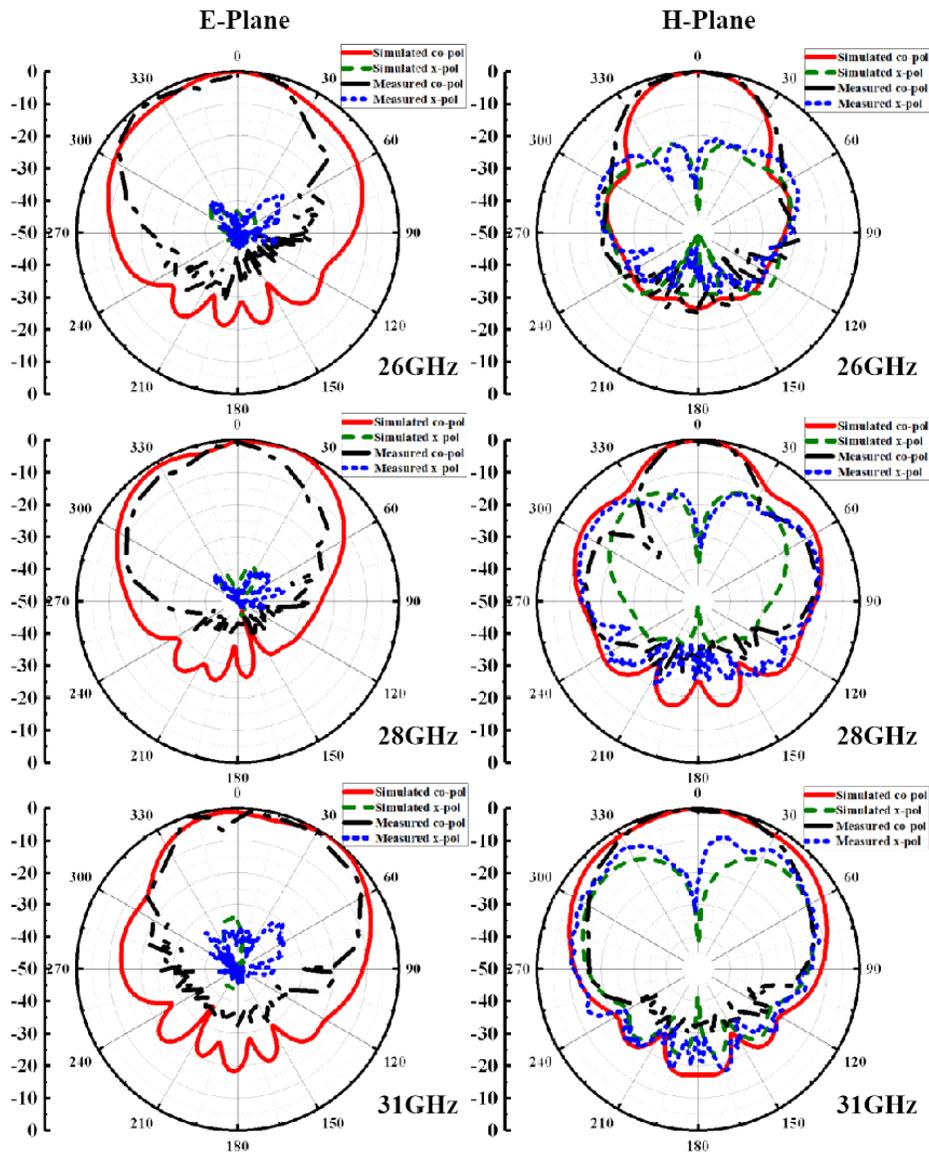
E-Plane   H-Plane

FIGURE 10. Simulated and measured radiation patterns at 26 GHz, 28 GHz, 31 GHz.

TABLE 2. Comparison of the proposed antenna with previously reported antenna.

Ref.	Antenna Type	Freq. (GHz)	BW (%)	Max. Gain (dBi)	Efficiency (%)	Size ($\lambda_0 \times \lambda_0 \times \lambda_0$)
[10]	Venus-shaped slot	60	9	9.65	–	$2.6 \times 1.8 \times 0.07$
[11]	Bow-tie slot	28	15.2	7	–	$0.75 \times 0.89 \times 0.07$
[13]	Slot and patch	27	14.4	7.5	84	$1.26 \times 1.26 \times 0.07$
[15]	Slot with Vias	10	20.8	5.7	84	$0.63 \times 1.07 \times 0.03$
[16]	Multiple slot	26	13.4	7.8	80	$1.59 \times 1.39 \times 0.04$
[18]	Patch fed by SIW	65	27	8.2	96	$0.67 \times 0.67 \times 0.38$
This work	Circular arc-shaped slot	28	20.9	11.5	85	$2.29 \times 1.87 \times 0.07$

decrease, and there is a clear downward trend in antenna efficiency. The possible reason is that the energy around the slot is not distributed in the main radiation direction because of the uneven distribution of energy around the slot. At the high frequency, the maximum radiation direction of the circu-

lar arc-shaped slot is shifted, resulting in the radiation in the high-frequency band generated by the feed inclined slot. In addition, dielectric loss and conductor loss greatly influence antenna radiation effect and transmission efficiency. Even if the selected dielectric material has a low dielectric loss, the energy
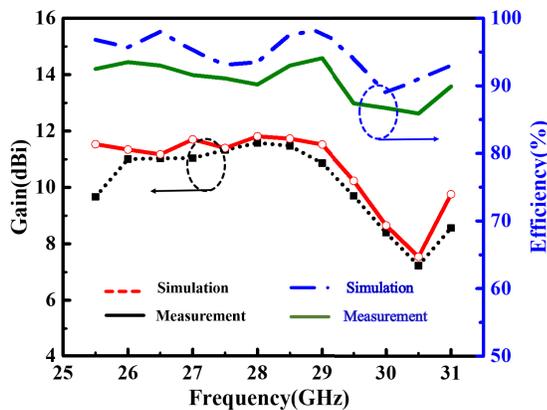
FIGURE 11. Measured and simulated gain and efficiency.

loss is inevitable at higher frequencies, so the antenna gain and efficiency are reduced under various factors.

Table 2 compares some published SIW antennas with this paper. As shown in Table 2, the antenna proposed in this paper can achieve a relative bandwidth of more than 20% at higher frequencies and has the advantages of high gain, low profile, simple structure, and easy fabrication.

4. CONCLUSION

A broadband circular arc-shaped slot antenna with SIW back cavity fed by GCPW is proposed in this paper. The interaction of the circular arc-shaped slot and the GCPW feeding structure helps to excite high-order modes, and the broadband impedance bandwidth can be obtained by making the high-order modes close to each other. Simulation and measurement results show that the antenna has good radiation characteristics and stable gain, achieving a wide impedance bandwidth of 22.6% and a peak gain of 11.5 dBi in the frequency range of 25.1–31.5 GHz. Due to its simple antenna construction, planar structure, high gain, and broad bandwidth, the developed antenna is ideal for broadband millimeter-wave communication systems.

REFERENCES

[1] Lockie, D. and D. Peck, "High-data-rate millimeter-wave radios," *IEEE Microwave Magazine*, Vol. 10, No. 5, 75–83, Aug. 2009.

[2] Rappaport, T. S., Y. Xing, G. R. MacCartney, A. F. Molisch, E. Mellios, and J. Zhang, "Overview of millimeter wave communications for fifth-generation (5G) wireless networks — With a focus on propagation models," *IEEE Transactions on Antennas and Propagation*, Vol. 65, No. 12, 6213–6230, Dec. 2017.

[3] Ali, M., K. K. Sharma, R. P. Yadav, A. Kumar, F. Jiang, Q. S. Cheng, and G.-L. Huang, "Design of dual mode wideband SIW slot antenna for 5G applications," *International Journal of RF and Microwave Computer-Aided Engineering*, Vol. 30, No. 12, e22449, 2020.

[4] Xiao, Z., Y. Pan, X. Liu, and K. W. Leung, "A wideband magnetoelectric dipole antenna with wide beamwidth for millimeter-wave applications," *IEEE Antennas and Wireless Propagation Letters*, Vol. 22, No. 4, 918–922, 2023.

[5] Chen, M., X.-C. Fang, W. Wang, H.-T. Zhang, and G.-L. Huang, "Dual-band dual-polarized waveguide slot antenna for SAR applications," *IEEE Antennas and Wireless Propagation Letters*, Vol. 19, No. 10, 1719–1723, 2020.

[6] Xu, F. and K. Wu, "Guided-wave and leakage characteristics of substrate integrated waveguide," *IEEE Transactions on Microwave Theory and Techniques*, Vol. 53, No. 1, 66–73, 2005.

[7] Luo, G. Q., Z. F. Hu, L. X. Dong, and L. L. Sun, "Planar slot antenna backed by substrate integrated waveguide cavity," *IEEE Antennas and Wireless Propagation Letters*, Vol. 7, 236–239, 2008.

[8] Luo, G. Q., Z. F. Hu, W. J. Li, X. H. Zhang, L. L. Sun, and J. F. Zheng, "Bandwidth-enhanced low-profile cavity-backed slot antenna by using hybrid SIW cavity modes," *IEEE Transactions on Antennas and Propagation*, Vol. 60, No. 4, 1698–1704, 2012.

[9] Chaturvedi, D., A. A. Althuwayb, and A. Kumar, "Bandwidth enhancement of a planar SIW cavity-backed slot antenna using slot and metallic-shorting via," *Applied Physics A*, Vol. 128, No. 3, 193, 2022.

[10] Mungaru, N. K. and S. Thangavelu, "Broadband substrate-integrated waveguide venus-shaped slot antenna for V-band applications," *Microwave and Optical Technology Letters*, Vol. 61, No. 10, 2342–2347, 2019.

[11] Li, H., Y. Cheng, L. Mei, and F. Wu, "Dual-polarized frame-integrated slot arrays for 5G mobile handsets," *IEEE Antennas and Wireless Propagation Letters*, Vol. 19, No. 11, 1953–1957, 2020.

[12] Cheng, T., W. Jiang, S. Gong, and Y. Yu, "Broadband SIW cavity-backed modified dumbbell-shaped slot antenna," *IEEE Antennas and Wireless Propagation Letters*, Vol. 18, No. 5, 936–940, 2019.

[13] Kumar, L., V. Nath, and B. Reddy, "A wideband substrate integrated waveguide (SIW) antenna using shorted vias for 5G communications," *AEU-International Journal of Electronics and Communications*, Vol. 171, 154879, 2023.

[14] Shi, Y., J. Liu, and Y. Long, "Wideband triple- and quad-resonance substrate integrated waveguide cavity-backed slot antennas with shorting vias," *IEEE Transactions on Antennas and Propagation*, Vol. 65, No. 11, 5768–5775, 2017.

[15] Wu, Q., J. Yin, C. Yu, H. Wang, and W. Hong, "Broadband planar SIW cavity-backed slot antennas aided by unbalanced shorting vias," *IEEE Antennas and Wireless Propagation Letters*, Vol. 18, No. 2, 363–367, 2019.

[16] Shi, Y., W. J. Wang, and T. T. Hu, "A transparent SIW cavity-based millimeter-wave slot antenna for 5G communication," *IEEE Antennas and Wireless Propagation Letters*, Vol. 21, No. 6, 1105–1109, 2022.

[17] Altaf, A., W. Abbas, and M. Seo, "A wideband SIW-based slot antenna for D-band applications," *IEEE Antennas and Wireless Propagation Letters*, Vol. 20, No. 10, 1868–1872, 2021.

[18] Mohamed, I. M. and A.-R. Sebak, "60 GHz 2-D scanning multi-beam cavity-backed patch array fed by compact SIW beamforming network for 5G applications," *IEEE Transactions on Antennas and Propagation*, Vol. 67, No. 4, 2320–2331, 2019.

[19] Wang, R., Y. Duan, Y. Song, W.-G. Zhao, Y.-H. Lv, M.-S. Liang, and B.-Z. Wang, "Broadband high-gain empty SIW

cavity-backed slot antenna," *IEEE Antennas and Wireless Propagation Letters*, Vol. 20, No. 10, 2073–2077, 2021.

[20] Liu, C.-M., S.-Q. Xiao, and K. Wu, "Wideband slot antenna backed by cylindrical substrate-integrated waveguide cavity," *IEEE Transactions on Antennas and Propagation*, Vol. 67, No. 3, 1509–1518, 2019.